LWT - Food Science and Technology 213 (2024) 117034

Contents lists available at ScienceDirect

LWT

journal homepage: www.elsevier.com/locate/lwt

Control of *Bacillus cereus* in rice cake and food contact surfaces with novel *Becedseptimavirus* genus phage BCC348 and its partial SPOR domain-containing endolysin LysBCC348

Hanbin Seol [a], Byoung Sik Kim [b,**], Minsik Kim [a,c,*]

[a] Laboratory of Molecular Food Microbiology, Department of Food and Nutrition, Brain Korea 21 FOUR, College of Human Ecology, Yonsei University, Seoul, 03722, South Korea
[b] Department of Food Science and Biotechnology, College of Engineering, Ewha Womans University, Seoul, 03760, South Korea
[c] POSTECH Biotech Center, Pohang University of Science and Technology (POSTECH), Pohang, 37673, South Korea

ARTICLE INFO

Keywords:
Alternative antimicrobial
Bacillus cereus
Bacteriophage
Becedseptimavirus
Endolysin
Garaetteok
SPOR domain

ABSTRACT

Here, we investigated the novel bacteriophage BCC348 and its endolysin LysBCC348 as alternative antimicrobials against the major foodborne pathogen *Bacillus cereus*. The *Becedseptimavirus* genus phage BCC348 effectively inhibited the growth of *B. cereus* ATCC 27348 with a remarkable burst size of ~600 PFU/infected cell. The cation-dependent amidase endolysin LysBCC348 lysed the host *B. cereus* and *Listeria monocytogenes* and EDTA-treated Gram-negative pathogens. In a cold storage model of Korean rice cake, *Garaetteok*, BCC348 significantly reduced artificially contaminated *B. cereus* counts to undetectable levels within 3 days. Treatment with LysBCC348 also achieved a ~1.3-log reduction of *B. cereus* and ~60% biofilm removal from food contact surfaces. Genes related to DNA modification and sporulation prevention in BCC348, as well as a partial sporulation-related repeat (SPOR) domain in LysBCC348, are thought to enhance the efficacy of BCC348 in controlling *B. cereus*. These results suggest that BCC348 and LysBCC348 are promising alternative candidates to mitigate *B. cereus* contamination in the food industry.

1. Introduction

Bacillus cereus is a ubiquitous environmental pathogen that is commonly found in various foods, including rice, vegetables, and processed meats. By producing emetic and diarrheal toxins, endospores, and forming biofilms on food contact surfaces, *B. cereus* has been identified as a major causative agent in several foodborne illness outbreaks, accounting for 1.4–12% of foodborne illnesses worldwide (Bottone, 2010; Grutsch et al., 2018; Huang et al., 2020). In general, starchy foods such as cooked rice and rice-based products, noodles, and pastries have been primarily associated with outbreaks of emetic *B. cereus* (Park & Yoon, 2019; Stenfors Arnesen et al., 2008).

Heating to high temperatures, electron beam irradiation, and the use of chemical sanitizers such as chlorine and ethanol have been investigated to address *B. cereus* issues in the food industry (Kim et al., 2019; Zhang et al., 2020). However, these physical and chemical methods are often less preferred due to detrimental effects on food quality, higher processing costs, and health concerns about residual chemicals. As consumers demand increases for minimally processed foods due to the perceived benefits of natural taste and nutritional value (Song et al., 2022), the development of alternative methods to selectively control harmful pathogens at affordable costs has become more necessary.

Bacteriophages, viruses that specifically infect bacteria, are increasingly investigated as alternative antimicrobials due to their specific lytic activity against target bacteria (Strathdee et al., 2023). Infection with prey bacteria leads to the synthesis of new infectious progeny within the host cell, and the progeny are released by host lysis

Abbreviations: CBD, cell-wall binding domain; EAD, enzymatically active domain; EOP, efficiency of plating; MOI, multiplicity of infection; PG, peptidoglycan; SM, sodium chloride-magnesium sulfate; SPOR, sporulation-related repeat.

* Corresponding author. Laboratory of Molecular Food Microbiology, Department of Food and Nutrition, Brain Korea 21 FOUR, College of Human Ecology, Yonsei University, Seoul, 03722, South Korea.
** Corresponding author.
E-mail addresses: b.kim@ewha.ac.kr (B.S. Kim), m.kim@yonsei.ac.kr (M. Kim).

https://doi.org/10.1016/j.lwt.2024.117034
Received 13 September 2024; Received in revised form 27 October 2024; Accepted 7 November 2024
Available online 8 November 2024
0023-6438/© 2024 The Authors. Published by Elsevier Ltd. This is an open access article under the CC BY-NC-ND license (http://creativecommons.org/licenses/by-nc-nd/4.0/).

with bacteriolytic phage proteins, holin and endolysin (Liu et al., 2023). Relatively low production costs, due to their abundance and self-replicating traits, and the lack of reported serious side effects in humans are attractive advantages of phage applications (Loc-Carrillo & Abedon, 2011; Marongiu et al., 2022). Unlike chemical agents, phages do not directly affect the sensory characeristics of food or non-target normal microbiota in food (Endersen & Coffey, 2020). Several phage products have been developed and commercialized since the U.S. FDA approved their use as food additives (Monk et al., 2010). However, phage products specifically for controlling *B. cereus* are not yet widely commercialized with relatively limited *B. cereus*-infecting phage resources.

Endolysins have also been successfully applied to control various foodborne pathogens (Schmelcher & Loessner, 2016). Typically, endolysins derived from phages that infect Gram-positive bacteria have a modular structure: an enzymatic active domain (EAD) at the N-terminus and a cell-wall binding domain (CBD) at the C-terminus. By cleaving specific bonds within the peptidoglycan (PG) layers of the bacterial cell-wall, endolysins rupture infected bacteria at the end of the phage life cycle. When applied exogenously, endolysin can directly and rapidly lyse Gram-positive bacteria, including *B. cereus*, wihich lacks an outer membrane. The low likelihood of bacteria developing resistance to endolysins supports the promising use of endolysins as another alternative antimicrobial (C. Lee, Kim, & Kim, 2023). However, to expand the useful panels of endolysins, more comprehensive structural and domain composition studies of novel endolysins need to be continued.

In light of these considerations, the present study aimed to characterize a novel *B. cereus*-infecting phage BCC348 and its distinctive endolysin LysBCC348. Given their significant bacteriolytic activity observed *in vitro*, we further investigated their potential as alternative antimicrobial agents against *B. cereus* and its biofilm in a storage model using *Garaetteok*, a traditional Korean rice cake, and on food contact surfaces, stainless steel and polystyrene. In addition, the possible explanation for the strong *B. cereus*-lysing activity of BCC348 was discussed in the light of the analysis results of the phage genome and endolysin structure.

2. Materials and methods

2.1. Bacterial strains and growth conditions

The bacterial strains used in this study are listed in Table 1. Unless otherwise noted, bacteria were grown in LB medium (CM0996T, Oxoid, UK) at 37 °C with constant shaking. *Staphylococcus* strains were grown in TSB medium (CM0129, Oxoid, UK) instead. Chemicals were added to the media, if necessary: kanamycin (Km, 50 μg/mL), carbenicillin (Cb, 100 μg/mL), and IPTG (1 mM).

2.2. Bacteriophage isolation, purification, and propagation

Bacteriophages were isolated, purified, propagated, and prepared into stocks as previously described, with some modifications (Kim & Ryu, 2011; J. Lee, Kim, & Kim, 2023). Briefly, carrots purchased from a local market were homogenized with PBS and mixed with 2 × LB broth. *B. cereus* ATCC 27348 was inoculated before the mixture was incubated for 8 h. Phages in the filtered (0.22 μm-pore size filter) supernatant were purified by a sequential spotting assay on a *B. cereus* ATCC 27348 lawn. After propagation in *B. cereus* culture supplemented with $CaCl_2$ and $MgCl_2$ (10 mM each), phages were precipitated with PEG 6000, ultracentrifuged, and dialyzed to prepare phage stocks.

2.3. Characterization of phage BCC348

2.3.1. Transmission electron microscopy

As previously described (J. Lee et al., 2023; Lee et al., 2023), the morphology of BCC348 was observed under a TEM (LIBRA 120, Carl Zeiss, Germany) after negative staining with 2% aqueous uranyl acetate. The virion lengths in the images were measured using ImageJ ($n = 10$).

Table 1
Bacterial strains used in this study.

Bacteria[a]		ϕBCC348[b]	LysBCC348[c]
Bacillus cereus	ATCC 14579	+++	++
	ATCC 10876	+++	++++
	ATCC 10987	–	++++
	ATCC 13061	I	++++
	ATCC 21768	–	++++
	ATCC 21772	I	+++
	ATCC 27348	+++	++++
	barley isolate	–	+++
	brown rice isolate	–	++
	raw food isolate	++	++
	raw rice isolate	–	+
	wheat isolate	++	+++
	red pepper isolate	–	++
B. subtilis	ATCC 6051	–	++
	ATCC 23857	–	–
Other Gram-positive bacteria			
Staphylococcus aureus	RN 4220	–	–
	ATCC 29213	–	–
Listeria monocytogenes	ATCC 19114	–	+++
L. innocua		–	++
Gram-negative bacteria			
Cronobacter sakazakii	ATCC 29544	–	++
Escherichia coli	DH5α	–	+
	MG 1655	–	++
	BL21 (DE3)	n.d.	n.d.
	O157:H7 ATCC 43890	–	+
	O157:H7 ATCC 43894	–	–
Salmonella Typhimurium	LT2(c)	–	+
S. Enteritidis	ATCC 13076	–	+
Shigella boydii	IB 2474	–	++
Sh. dysenteriae	IB 2476	–	++++
Sh. flexneri	2a strain 24574	–	++++
Sh. sonnei	IB 707	–	++

[a] Gram-negative bacteria were pretreated with 100 mM EDTA. *E. coli* BL21 (DE3) was used for the protein expression.
[b] +++, 0.1<EOP ≤1; ++, 0.01<EOP≤0.1; +, EOP ≤0.01; I, inhibition zone; -, no plaque; n.d., not determined.
[c] Relative lytic activity compared to that against the indicator strain *B. cereus* ATCC 14579. -, 0–10%; +, 10–50%; ++, 50–100%; +++, 100–150%; ++++, 150% or more; n.d., not determined.

2.3.2. Determination of host range and EOP

Phages were serially diluted in SM buffer (50 mM Tris-HCl at pH 7.5, 100 mM NaCl, and 10 mM $MgSO_4$) and the dilutions were applied to bacterial lawns. After overnight incubation, the efficiency of plating (EOP) was calculated by dividing the number of plaques formed on each bacterial lawn tested by those on the *B. cereus* ATCC 27348 lawn.

2.3.3. Phage stability test

Phage stability was determined as described elsewhere, with some modification (Choi & Kim, 2021). For heat stability, phages (10^6 PFU/mL) were incubated at temperatures ranging from 4 to 80 °C in a heat block. For pH stability, phages suspended in LB media adjusted to pH values ranging from 2 to 12 were placed at 37 °C. After 1 h of treatment, the surviving phages were counted using a spotting assay.

2.3.4. Phage adsorption assay and one-step growth curve analysis

Phage adsorption to the host bacteria was examined as previously described (Choi & Kim, 2021), with a modification: $MgCl_2$ and $CaCl_2$ (10 mM each) were added along with phage infection at a multiplicity of infection (MOI) of 0.01. The phage adsorption rate was calculated as follows: [adsorption rate (%)] = $(P_t/P_0) \times 100$, where P_t, phage titer at time t (PFU/mL); P_0, initial phage titer determined from the bacteria-free control.

The one-step growth curve was analyzed as described elsewhere

(Kim et al., 2023). Briefly, *B. cereus* ATCC 27348 was infected with phages (MOI of 0.01) and supplemented with $CaCl_2$ and $MgCl_2$. After incubation at room temperature (RT) for 5 min, the culture was washed with fresh media and further incubated at 37 °C for up to 70 min. Samples were taken every 5 min and divided into two tubes, one containing 2% (v/v) chloroform. Samples were immediately diluted in SM buffer and the number of phages was counted by spotting assay. The PFU per infected cell at each time point was calculated by dividing the PFU at each time point by the PFU of the chloroform-free sample at 0 min.

2.3.5. Bacterial challenge assay

Exponentially growing *B. cereus* ATCC 27348 was infected with phages at various MOIs. During incubation with constant shaking for 12 h, bacterial growth was monitored periodically by measuring the absorbance at 600 nm (A_{600}) using a microplate reader (Spark®, Tecan, Switzerland).

2.4. Genomic and bioinformatic analysis

Phage genome was manually extracted using a previously described hot phenol/chloroform/isoamyl-alcohol method (Wilcox et al., 1996). The extracted genomic DNA was sequenced using an Illumina Miseq. sequencer (Illumina, San Diego, CA), and the sequence reads were *de novo* assembled using SPAdes (v.3.14.1) at Sanigen Inc. (Seoul, South Korea). Prediction of ORFs, tRNAs, and putative virulence factors in the assembled genome was made using several genomic analysis tools. Appropriate bioinformatic tools were also used for comparative analysis of genomes and proteins (*see Supplementary methods*). The complete genome sequence of BCC348 was deposited in NCBI GenBank (OK513034).

2.5. Cloning, expression, and purification of endolysins

The endolysin gene was PCR amplified using the appropriate oligonucleotides (Supplementary Table S1). Plasmid pET28a-eGFP was used as a template for eGFP amplification (Kong et al., 2015). The amplified DNA fragments were cloned into expression vectors, pET28b and pHIS-parallel1, using an isothermal assembly method (Gibson et al., 2009). *Escherichia coli* BL21 (DE3) was transformed with the constructed recombinant vector via electroporation.

To induce protein expression, IPTG-treated, transformed *E. coli* was incubated at 18 °C for 20 h. Cells were then harvested and disrupted in lysis buffer (50 mM NaH_2PO_4, 300 mM NaCl, 10 mM imidazole, pH 8.0) by sonication (Digital Sonifier SFX450, Branson Ultrasonics). The filtered supernatant containing soluble proteins was applied to Ni-NTA affinity chromatography (Ni-NTA agarose, Qiagen, CA) prior to elution of target His_6-tagged proteins with elution buffer (lysis buffer containing 500 mM imidazole). Before storage of purified proteins at 4 °C, the buffer was exchanged with storage buffer (50 mM NaH_2PO_4, 300 mM NaCl, pH 8.0) using PD-Miditrap G-25 according to the manufacturer's instructions (Cytiva, Waukesha). Protein purification was confirmed by SDS-PAGE. If necessary, proteins were purified with FPLC (ÄKTA avant 25, cytiva, Sweeden; NFEC-2024-10-300227).

2.6. Characterization of endolysin LysBCC348

2.6.1. Lytic activity determination

The bacteriolytic activity of endolysin was determined by a turbidity reduction assay as previously described (Kim et al., 2024). Briefly, bacterial cells were resuspended in reaction buffer (50 mM NaH_2PO_4, 300 mM NaCl, pH 8.0) to adjust the optical density at 600 nm (OD_{600}) to 1.0. For Gram-negative bacteria, cells were pretreated with 0.1 M EDTA and 20 mM Tris-Cl (pH 8.0) for 5 min. After endolysin treatment, OD_{600} was monitored over time at RT. An endolysin-free cell suspension served as a control. The relative lytic activity was calculated as follows (Wan et al., 2021): [relative lytic activity (%)] = [(decrease in OD_{600} of endolysin-treated group – decrease in OD_{600} of control)/initial OD_{600} of control] × 100. The rate of lytic activity was calculated as the drop in milli-optical density per minute (-mOD_{600}/min) using 1.5 μM of enzyme.

2.6.2. Determination of thermostability and optimal reaction conditions

To test thermostability, LysBCC348 (5 μM) was incubated at temperatures ranging from −20 to 60 °C for 1 h, and its lytic activity was determined over 2 h as described in *section 2.6.1*. To determine the optimal pH for bacteriolytic activity, *B. cereus* cells suspended in reaction buffer adjusted to pH 2 to 12 were treated with LysBCC348 for 2 h, and then the lytic activity was compared. The optimal NaCl concentration for LysBCC348 activity was determined similarly by comparing lytic activity in reaction buffer with NaCl concentrations from 0 to 1000 mM over 2 h.

2.6.3. Determination of metal ion dependency

The effect of metal ions on lytic activity was determined as previously described (Son et al., 2012). LysBCC348 was incubated with 5 mM EDTA at 37 °C for 1 h to chelate metal ions. After buffer exchange with reaction buffer, the lytic activity of the EDTA-treated LysBCC348 on cell suspensions containing metal ions (0.1 mM of $ZnCl_2$, $MgCl_2$, $MnCl_2$, $CuCl_2$, or $CaCl_2$, final concentration) was evaluated for 1 h.

2.7. Model applications of BCC348 and LysBCC348

2.7.1. Application of BCC348 in a storage model of Garaetteok

Garaetteok is a traditional Korean rice cake made by soaking rice grains in water, grinding them into powder, making a dough, steaming it, and extruding it into a long cylindrical shape (Ku et al., 2018). The hot extruded *Garaetteok* is then immediately immersed in cold water and dried at 4 °C for about 5 days, but contamination often occurs after cooling, posing a threat to consumers. To simulate this final part of the production process, *Garaetteok* purchased from a retail market was re-steamed for 20 min, immediately immersed in cold sterilized distilled water (D.W.), dried in a laminar-flow biosafety cabinet (BSC) for 1 h, and then inoculated with *B. cereus* ATCC 27348 (10^7 CFU/25 g of rice cake) using an atomizer. After 1 h, phage BCC348 was sprayed onto the *Garaetteok* (MOI of 10 or 100). During storage at 4 °C for 3 days, a piece of *Garaetteok* was sampled daily. The bacterial count on the sampled *Garaetteok* was measured by homogenizing the sample in 0.1% peptone water with a stomacher (BagMixer 400, Interscience, France), serially diluting the filtered homogenates in PBS, and plating the dilutions on fresh LB plates.

2.7.2. Application of LysBCC348 in models of food contact surfaces

The effect of LysBCC348 on *B. cereus*-contaminated stainless steel was assessed as described elsewhere with modifications (Kim et al., 2024). Autoclaved stainless steel coupons were spiked with *B. cereus* cell suspension (10^9 CFU/mL) and dried in a BSC for 1.5 h at RT. LysBCC348 was then treated for 2 h at RT. Reaction buffer was used as a control instead. After treatments, the remaining cells on the coupon surface were collected with PBST (PBS containing 0.05% Tween 20 [v/v]) and counted by plating on LB plates.

The biofilm removal efficacy of LysBCC348 was determined as described previously with modifications (Zhao et al., 2021). Briefly, *B. cereus* ATCC 10987, known as a strong biofilm producer (Okshevsky et al., 2018), was grown in TSB with 0.5% yeast extract in a 96-well polystyrene microplate (No. 32096, SPL, South Korea) at 30 °C for 48 h without aeration. After washing with D.W., the biofilm was treated with LysBCC348 for 3 h. The amount of biofilm was then quantified by staining with 1% crystal violet for 15 min, washing three times with D.W., eluting the stains with 33% acetic acid, and measuring the OD_{570} of the elutes. The relative biofilm removal activity was calculated as follows: [relative removal activity (%)] = (OD_{570} of endolysin-treated group/OD_{570} of reaction buffer-treated control) × 100.

2.8. Statistical analysis

Results of independent triplicate experiments are presented as mean with standard deviation (s.d.), unless otherwise noted. Statistical analysis was performed using Student's *t*-test or one-way ANOVA with Tukey's multiple comparison post-hoc test, using GraphPad Prism v8.4.3 (GraphPad Software, CA) for statistical analysis. *P*-values less than 0.05 were considered statistically significant.

3. Results

3.1. Novel phage BCC348 as a potent anti-B. cereus agent

Phage BCC348 formed small but clear plaques on host *B. cereus* ATCC 27348 lawn (Fig. 1A). TEM analysis revealed that BCC348 had an isomeric head and a long, contractile tail (Fig. 1B). The diameter of the head was approximately 78.00 ± 4.05 nm ($n = 10$), and the length of the tail was 259.12 ± 5.87 nm ($n = 10$, extended form) and 100.81 ± 19.3 nm ($n = 3$, contracted form).

Since stability is a critical factor for phage application, the stability of BCC348 was assessed under various conditions. The titer of BCC348 was stable between 4 and 50 °C, but decreased significantly at 60 °C ($P < 0.05$) and was completely below a limit of detection (LOD) at 70 °C (Fig. 1C). Phage infectivity was detected between pH 5 and 10, but was below the LOD below pH 4 and above pH 11 (Fig. 1D).

Within the first 5 min of infection, approximately 55.7% of the BCC348 bound to the host *B. cereus* (Fig. 1E). Within the next 25 min, up to approximately 70% of the virions slowly attached to the host, while 100% were still present as free particles in the bacteria-free control. In the one-step growth, newly synthesized BCC348 appeared within the infected host cell at 20 min (eclipse period), and the amplified BCC348 particles were released from the host cells at 40 min of infection (latent period). The burst size was calculated to be approximately 604 PFU per infected single host cell (Fig. 1F).

A remarkable growth inhibition of *B. cereus* ATCC 27348 was observed *in vitro* by BCC348 treatment (Fig. 1G). Compared to the phage-free, SM buffer-treated control, when the phage was added at an MOI of 0.1, *Bacillus* growth began to be inhibited at 1.5 h post-infection, and the growth was completely inhibited from 3 to 7 h post-infection. At MOIs of 1 and 10, *B. cereus* was unable to grow from the start. Although growth resumption was detected after 7.5 h at MOIs of 0.1 and 1, no bacterial growth was observed up to 12 h at an MOI of 10. Taken together, the clear plaques, large burst size, and long-lasting bacterial inhibitory activity suggest the potential of BCC348 as an antimicrobial agent for *B. cereus* control.

3.2. Proposal of BCC348 as a second member of the genus Becedseptimavirus

Genomic analysis revealed that the 94,623-bp dsDNA genome of BCC348 contained a total of 150 ORFs, of which 116 were hypothetical proteins of unknown function (Supplementary Fig. S1 and Table S2). The gene products of the remaining ORFs were classified into six groups based on their function: DNA synthesis/manipulation, packaging, host lysis, structure, transcription, and additional functions such as a putative stage V sporulation protein S (SpoVS) gene and preQ$_0$ biosynthesis genes. No tRNA genes were found. Neither bacterial virulence nor toxin genes nor lysogenic cycle-related genes were predicted, supporting the safety of BCC348 as a *B. cereus*-control agent. The inability of BCC348 to lysogenize *B. cereus* was further confirmed by the lysogen activity assay (*see Supplementary methods*, Fig. S2 and Table S3).

Phylogenetic analysis based on the terminase large subunit (TerL) revealed that BCC348, along with another *B. cereus* phage BCD7 (Genbank accession No. NC_019515), formed a distinct clade from other *Bacillus*-infecting phages (Fig. 2A). The TerL of BCC348 shared the highest homology (99.62% identity) with that of BCD7, but had low homology (<25% identity) with that of other *B. cereus* phages. Pairwise comparison of the whole genome using BLASTn showed that the BCC348

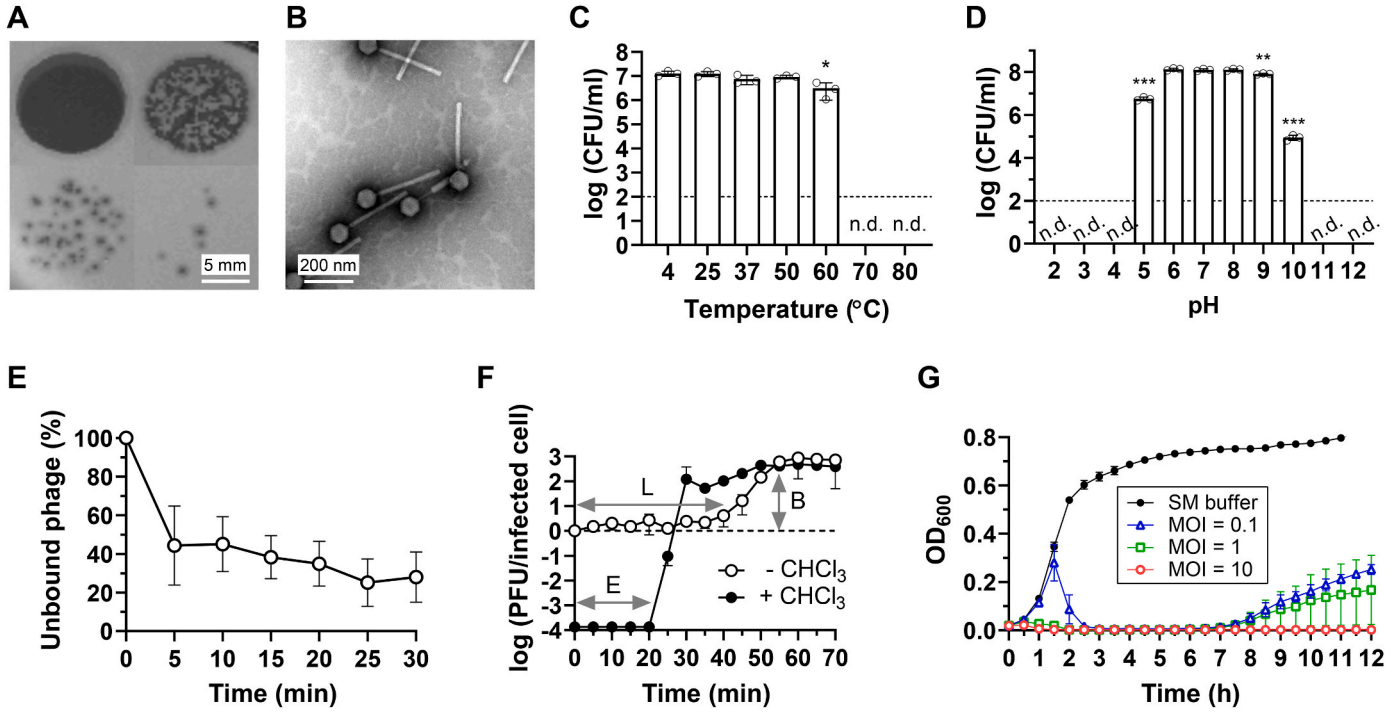


Fig. 1. Characteristics of novel bacteriophage BCC348. (A) Plaque morphology of BCC348 on the lawn of host *B. cereus* ATCC 27348. **(B)** TEM image of BCC348. **(C and D)** The number of surviving infectious BCC348 after exposure to ranges of indicated **(C)** temperatures and **(D)** pH. **(E)** Adsorption of BCC348 to host *B. cereus* ATCC 27348. **(F)** One-step growth curve of phage BCC348 in a single infected *B. cereus* ATCC 27348 cell. $CHCl_3$, chloroform; E, eclipse period; L, latent period; B, burst size. **(G)** Bacterial challenge assay of *B. cereus* ATCC 27348 with BCC348 at the indicated MOIs. Statistical differences were analyzed by comparing the results with that of 4 °C in **(C)** and pH 6 in **(D)**. *, $P < 0.05$; **, $P < 0.01$; ***, $P < 0.001$; n.d., not detected; dashed line, limit of detection (LOD).

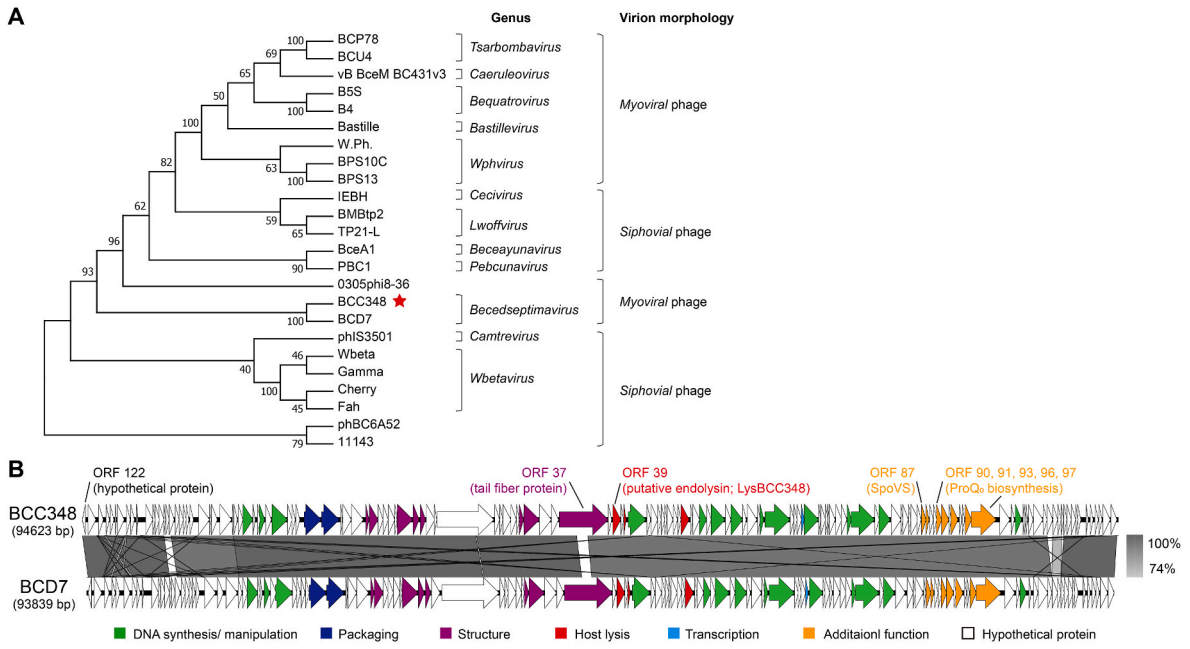


Fig. 2. Genomic characteristics of BCC348. **(A)** Phylogenetic tree of *B. cereus* phages based on the amino acid sequence of the terminase large subunit. The bootstrap probabilities are indicated at the nodes. Genus and virion morphologies are also shown, if reported. Accession number and additional taxonomic information for each protein are listed in Table S4. **(B)** Comparison of BCC348 and BCD7 genomes. Functional categorization of putative gene products is color-coded as indicated in the legends. Note that the BCC348 genome has been rearranged to facilitate comparison with the BCD7 genome.

genome shared 96.97% similarity with the BCD7 genome (Fig. 2B). The difference was found in three regions, two in hypothetical proteins (ORFs 138–139 and 107–110) and one in a tail fiber protein (ORF 37). Only phages with less than 1% query coverage to the BCC348 genome were identified in the BLAST search results, indicating the absence of other similar phages. Based on these results, we propose that BCC348

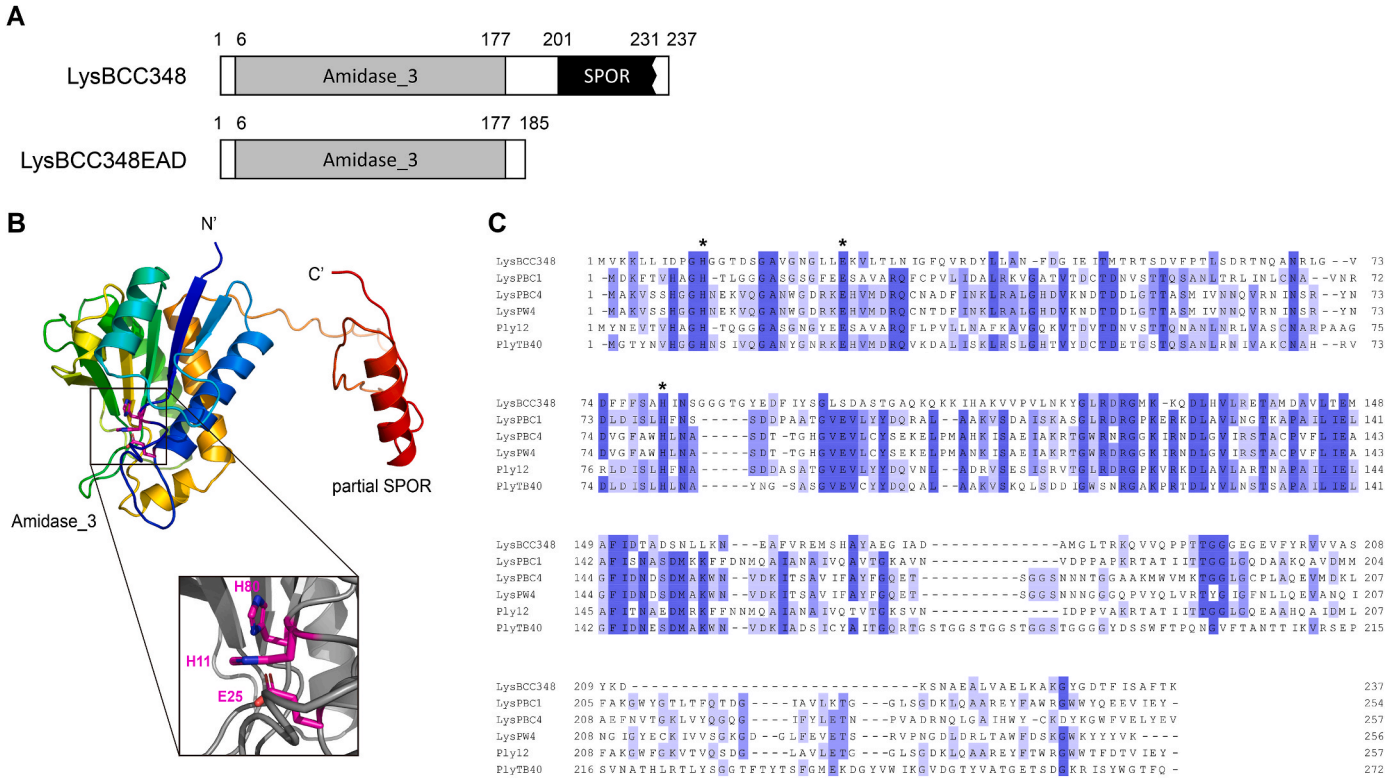


Fig. 3. Structural analysis of endolysin LysBCC348. **(A)** Schematic diagrams of LysBCC348 and LysBCC348EAD. **(B)** The deduced 3D model of LysBCC348 using AlphaFold 3. The inset represents three conserved metal ion binding sites. **(C)** Sequence alignment of LysBCC348 with other *B. cereus*-lysing endolysins containing the Amidase_3 domain. Amino acid sequences were retrieved from the NCBI Genbank as follows: LysPBC1, accession No. AFE86261.1, LysPBC4, AKQ08217; LysPW4, AZU99073; Ply12, Y11476; and PlyTB40, ALA13156. The asterisks indicate the conserved metal ion binding site in *N*-acetylmuramoyl-L-alanine amidase.

belongs to the genus *Becedseptimavirus*, to which phage BCD7 alone belonged.

3.3. LysBCC348, a putative endolysin with an unusual C-terminal partial SPOR domain

Among the annotated ORFs of BCC348, two (ORF 39 and 51) were predicted to be associated with host lysis (Fig. 2). The gene product of ORF 51 (Gp51) is predicted to contain a mannosyl-glycoprotein endo-β-*N*-acetylglucosaminidase domain (PF01832), an enzymatic domain that catalyzes the cleavage of the bond between *N*-acetylglucosamine (GlcNAC) and *N*-acetylmuramic acid (MurNAc) in the cell wall PG layers. However, no bacteriolytic activity was observed against *Bacillus* with the purified Gp51 (Fig. S3).

The gene product of ORF 39, designated LysBCC348, was predicted to contain an *N*-acetylmuramoyl-L-alanine amidase domain that cleaves the bond between MurNAc and L-alanine of the PG. The Amidase_3 domain (PF01520) was found at the N-terminus as a typical EAD, similar to other modular endolysins (Fig. 3A and B). Metal ion binding sites (His11, Glu25, and His80) were identified in the Amidase_3 domain, which is well conserved in other *B. cereus*-lysing endolysins (Fig. 3C). However, at the C-terminus, a partial sporulation-related repeat (SPOR) domain (PF05036) was present as an unusual CBD motif (Oliveira et al., 2013), suggesting the novelty of LysBCC348.

When purified LysBCC348 (Fig. S4A) was applied, the turbidity of the *B. cereus* suspension was significantly reduced in a dose-dependent manner (Fig. 4A top). Treatment with the reaction buffer (i.e., 0.00 μM of LysBCC348) did not significantly affect the suspension's turbidity. However, treatment with 1.5 μM LysBCC348 lysed the cells rapidly, resulting in a halving of turbidity within 1 h, and the lysis continued before reaching a plateau at ~3 h. The number of viable cells was also immediately reduced by 1-log with LysBCC348 treatment, and approximately a 2-log reduction was achieved after 3 h (Table 2).

When LysBCC348EAD, a truncated form containing only EAD, was applied, the activity was attenuated (Fig. 4A bottom and Fig. S4B). During the first 3 h of treatment, even at a high concentration (i.e., 1.5 μM), turbidity was not significantly reduced. However, the cells were then lysed in a dose-dependent manner, and the reduction comparable to that of LysBCC348 was achieved with 1.5 μM LysBCC348EAD after 9 h. The rate of lytic activity was faster for LysBCC348 than for LysBCC348EAD (5.19 ± 0.11 vs. 2.61 ± 0.02). These results suggest that the unusual partial SPOR domain at the C-terminus plays a role in enabling LysBCC348 to function fully as an endolysin for phage BCC348, despite the absence of the typical CBD.

Table 2
Reduction of viable *B. cereus* cells by LysBCC348 treatment.

	Reaction buffer control		LysBCC348	
	0 h	3 h	0 h	3 h
B. cereus (CFU/mL)	(1.05 ± 0.59) × 10^7	(2.37 ± 0.65) × 10^7	(4.43 ± 1.1) × 10^6	(6.43 ± 1.2) × 10^5

3.4. Optimal conditions for lytic activity of cation-dependent LysBCC348

The lytic activity of LysBCC348 was maintained from −20 to 40 °C and decreased to less than 15% activity at 50 °C compared to that observed at 20 °C (Fig. 4B). The activity was completely lost at 60 °C, indicating thermal inactivation. The highest activity was observed at 200 mM NaCl, and the activity decreased with increasing or decreasing NaCl concentration (Fig. 4C). Remarkably, even at 1000 mM concentration, the activity remained substantial at ~40% compared to the highest activity at 200 mM NaCl. The lytic activity was highest at pH 9 and decreased significantly with either decreasing or increasing pH (Fig. 4D). The activity completely disappeared at pH values below 4 and above 11, indicating that the highly acidic and basic conditions were detrimental to LysBCC348.

Consistent with the presence of metal-binding sites in the Amidase_3 domain (Fig. 3C), approximately 95% of the lytic activity was lost when the metal ions were chelated with 5 mM EDTA (Fig. 4E). However, the lost activity was restored by adding 0.1 mM of various divalent cations to the reaction buffer. Notably, approximately 90% of the activity was

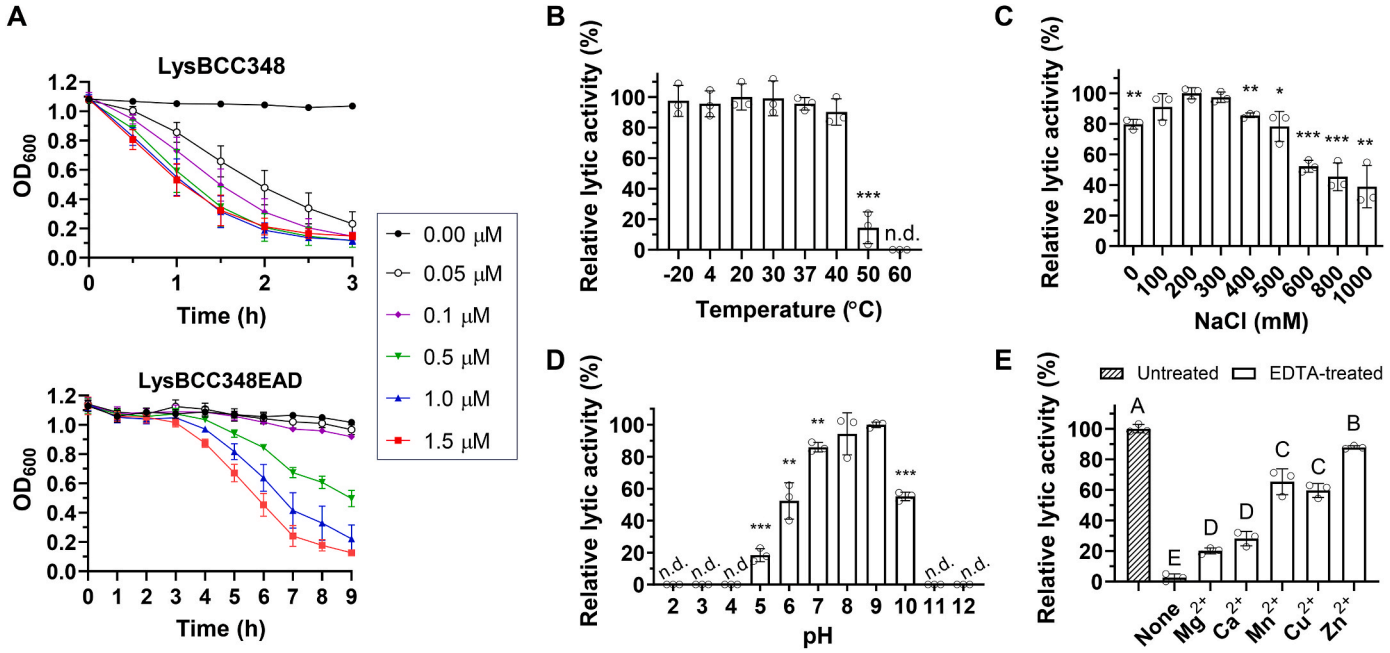


Fig. 4. Characteristics of LysBCC348. **(A)** Lytic activity of LysBCC348 and LysBCC348EAD by the turbidity reduction assay. **(B)** Thermal stability of LysBCC348. **(C and D)** Effect of NaCl concentration **(C)** and pH **(D)** on the lytic activity of LysBCC348. **(E)** Effect of metal cations on the lytic activity of LysBCC348. Relative lytic activity was calculated by comparison with the lytic activity of LysBCC348 at 20 °C in **(B)**, at 200 mM NaCl in **(C)**, at pH 9 in **(D)**, or without EDTA treatment (untreated) in **(E)**. Statistical differences were analyzed by using Student's *t*-test **(B–D)** or one-way ANOVA **(E)**. *, $P < 0.05$; **, $P < 0.01$; ***, $P < 0.001$; n.d., not detected. The capital letters above the columns indicate significant differences ($P < 0.05$) between the test groups.

restored by Zn^{2+}.

3.5. Controllable bacterial range by BCC348 and LysBCC348

To compare the controllable range of BCC348 and LysBCC348, their antimicrobial activity was tested with various Gram-positive and -negative bacteria (Table 1). Five different *B. cereus* strains tested, including two food isolates, were susceptible to BCC348, while *B. subtilis* and other Gram-positive and -negative strains were not. LysBCC348 showed a much broader controllable range than BCC348. All thirteen *B. cereus* strains tested, including six food isolates, and two Gram-positive *Listeria* spp. including *Listeria monocytogenes* were lysed by LysBCC348. Remarkably, panels of Gram-negative bacteria, including notorious foodborne pathogens, were also susceptible to LysBCC348 when their outer membrane was permeabilized by 100 mM EDTA treatment. The reproducibility of these results was confirmed across at least three independent trials.

3.6. Applications in food and food contact surface models

Because *B. cereus* food poisoning is often associated with starchy foods, steamed *Garaetteok*, a traditional Korean rice cake, was used as a representative model of food contaminated with *B. cereus*. When BCC348 was treated at MOIs of 10 and 100, the number of *B. cereus* cells artificially spiked into the steamed *Garaetteok* gradually decreased during refrigerated storage (Fig. 5A). An approximate 1-log reduction also occurred in the control SM buffer-treated group, probably due to the low temperature, but a more significant and rapid reduction was achieved with BCC348 treatment ($P < 0.05$). *B. cereus* cells below the LOD were observed three days after the phage treatment.

Since stainless steel is a common surface material for food processing equipment, including extruders for *Garaetteok* production, the potency of LysBCC348 in controlling *B. cereus* adhesion to stainless steel surfaces was evaluated. Compared to the negative control with only reaction buffer, the LysBCC348-treated groups reduced the number of adherent *B. cereus* cells on stainless steel (Fig. 5B). Approximately 1.1-log or more reduction was achieved with 0.5 μM or more LysBCC348 within 2 h.

Next, the potential of LysBCC348 to remove *B. cereus* biofilm from the surface of polystyrene, a widely used material for food utensils and containers, was investigated. *B. cereus* biofilm was removed by approximately 40% with 0.5 μM LysBCC348 treatment, and ~60% removal was achieved with more than 1 μM endolysin ($P < 0.05$) (Fig. 5C).

4. Discussion

A novel myoviral phage BCC348 isolated and characterized here showed many promising and intriguing aspects as an alternative anti-*B. cereus* candidate. Particularly, the large burst size of BCC348 explains its efficacy against the target *B. cereus*. BCC348 produced an average of ~600 phages per single infected cell, which is approximately 2–55 times higher than those of other previously reported *B. cereus* phages DZ1, vB_BceP_LY3, FWLBc1, and FWLBc2 (Huang et al., 2024; Lee et al., 2011; Tan et al., 2024). Due to this enormous progeny production in a single infection cycle, BCC348 treatment could provide immediate and effective control of *B. cereus* without growth resumption, both *in vitro* culture for up to 12 h and in the starchy food model, *Garaetteok*, for up to 3 days. The other *B. cereus* phage DLn1 also has a large burst size of 618 PFU per infected cell and effectively reduced the number of contaminated *B. cereus* in milk at 25 °C within 6 h by more than 4-log, but *B. cereus* growth resumed (Li et al., 2022), in contrast to our BCC348 case, highlighting the potency of BCC348 as an attractive and effective option for *B. cereus* control.

The notable distinctiveness of BCC348 compared to other *B. cereus* phages was also represented in its genome and genes. BCC348 shared high nucleotide sequence identity (96.97%) with a previously reported but uncharacterized other *B. cereus* phage, BCD7 (GenBank accession no. NC_019515). BCD7 showed extremely low similarity to other previously isolated phages in terms of genomic context (Lee et al., 2014) and is therefore classified as a singleton member of the genus *Becedseptimavirus*. We propose BCC348 as the second member of this genus based on the high genomic similarity and their placement together in a distinct clade in the phylogenetic analysis. However, differences between the genomes of BCC348 and BCD7 were also noteworthy (Fig. 2). In particular, a low similarity was observed in the region of ORF 37 encoding a tail fiber protein (89% query coverage, 92.12% identity with the homolog of BCD7). Since phage tail fibers often serve as host determinants associated with recognition of host receptors (Dunne et al., 2021; Ouyang et al., 2024), this difference suggests the possibility of a different host range between BCC348 and BCD7 at the *Bacillus* species and/or strain level.

We categorized the unusual and distinguishing genes of the *Becedseptimavirus* genus phage BCC348 compared to others into the category of additional functions (Fig. 2B and Table S2). BCC348 ORF 57 encodes a SpoVS that interferes with the early stages of *Bacillus* spp. sporulation (Liu et al., 2021; Resnekov et al., 1995). We speculated that SpoVS in BCC348 may prevent *B. cereus* from differentiating into endospores, thereby maintaining infected *B. cereus* in a vegetative state to serve as viable cell factories for progeny production. Previously, Kong et al. also suggested that *B. cereus* phage PBC2 inhibits sporulation by degrading

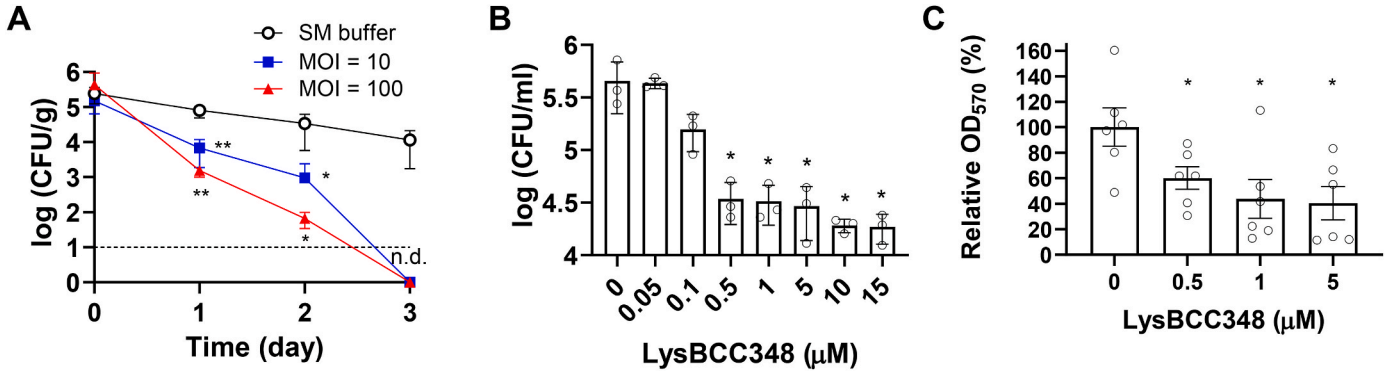


Fig. 5. Applications of BCC348 and LysBCC348 in food and food contact surface models. **(A)** Reduction of *B. cereus* contamination in *Garaetteok*, a traditional Korean rice cake, by BCC348 treatment. **(B)** Disinfection of *B. cereus* on a stainless steel surface by a 2 h treatment with LysBCC348. **(C)** Removal of *B. cereus* biofilm formed on the polyethylene surface by a 3 h treatment with LysBCC348. Sextuplicate results are presented in **(C)**. Statistical differences were analyzed by comparing the results with that of the SM buffer-treated control at each time point in **(A)** and the endolysin-untreated control in **(B)** and **(C)**. *, $P < 0.05$; **, $P < 0.01$; n.d., not detected; dashed line, limit of detection (LOD).

the forming spore cortex using a spore-binding domain (SBD)-containing endolysin because endospores are unproductive for phages (Kong et al., 2019). Whether the BCC348 SpoVS plays such an anti-sporulation role needs to be investigated in further studies. The BCC348 ORFs 90, 91, 93, 96, and 97 were analyzed as homologs of the $preQ_0$ biosynthesis genes *queD*, *queE*, *queC*, *folE*, and *tgt*, respectively. These genes have been reported to be involved in the 7-deazaguanine modification of DNA, thereby rendering the phage genome resistant to bacterial restriction enzymes (Hutinet et al., 2019; Thiaville et al., 2016; Weigele & Raleigh, 2016). The strikingly efficient inhibition of *B. cereus* by BCC348 may be related to the evasion of host restriction enzymes by these gene cluster-mediated genome modifications.

The endolysin LysBCC348, a protein of the *N*-acetylmuramoyl-L-alanine amidase family, showed remarkable lytic activity. A significant reduction of *B. cereus* and its biofilm on stainless steel and polystyrene surfaces by LysBCC348 treatment suggests its potential use as an alternative anti-*Bacillus* agent in the cleaning of food contact surfaces (Fig. 5B and C). Its stability, especially against temperatures up to 40 °C, a wide range of NaCl concentrations, and pH ranges between 6 and 10, also supports the usefulness of LysBCC348 in the food industry, where relatively harsh environmental conditions are common.

The partial SPOR domain at the C-terminus, where a typical modular endolysin possesses the CBD, is a striking feature of LysBCC348 (Fig. 3). Although the term 'SPOR' was derived from the early findings that proteins such as CwlC containing this small PG-binding domain participate in mother cell lysis during sporulation, SPOR domains are also frequently found in several bacterial cell division-related proteins, such as FtsN, DamX, and RlpA (Chen et al., 2018; Yahashiri et al., 2015, 2017). In the septal PG of the dividing cell, the SPOR domain-containing proteins bind to the denuded glycan strands, regions where the PG has lost peptide side chains due to cell wall amidase activities, and mediate their specific functions for cell division. Twenty-three endolysins possessing the SPOR domain have been retrieved from the phage lytic protein PhaLP database (Table S5), but none have yet been extensively characterized for the function of their SPOR domain in binding to the host cell or cell-wall (Criel et al., 2021).

The standard SPOR domain consists of two 35-residue tandem repeats, each consisting of two β-sheets and one α-helix in the βαβ order, which fold into a pseudo-2-fold symmetrical single-domain structure (Mishima et al., 2005; Williams et al., 2013). However, LysBCC348 possesses a partial SPOR domain of a single repeat with only one predicted α-helix structure (Fig. 3B and Fig. S5). To investigate whether this partial SPOR domain can serve as a CBD, an N-terminally eGFP-tagged version of the partial SPOR domain was expressed, and the binding to *B. cereus* was monitored by fluorescence microscopy. However, no binding to the target cells was observed, at least under the conditions tested (*see Supplementary methods*, Fig. S6). The binding capacity of the SPOR domain in CwlC to the PG was dependent on the two invariant conserved asparagine residues in each repeat, located at the edge of the domain in equivalent symmetric positions (Mishima et al., 2005). Thus, the non-observed binding of the LysBCC348 SPOR domain to *B. cereus* could be due to the absence of the secondary repeat in the domain. Nevertheless, removal of the SPOR domain significantly decreased LysBCC348's lysis activity and rate (Fig. 4A bottom), suggesting that the SPOR domain, with its putative but not elucidated contribution to host cell-wall binding, is necessary for the full activity of LysBCC348. By possessing this weak and partial SPOR domain in its endolysin, phage BCC348 may have had a sufficiently long latent period without premature host lysis, thereby being able to produce an enormous amount of progeny from the infected host cell (Fig. 1F). Whether the addition of a secondary repeat to the SPOR domain can enhance the lytic activity of LysBCC348 requires to be investigated in further studies.

LysBCC348 showed a broader spectrum of controllable targets than BCC348 (Table 1). Not only *B. cereus*, but also other Gram-positive *B. subtilis* and *L. monocytogenes* and even EDTA-treated Gram-negative bacteria were lysed by LysBCC348. Because the PG type of *Bacillus* and *Listeria* is the A1γ-variant, and most Gram-negative bacteria also have the same type of cell wall, LysBCC348 can lyse such a wide range of bacteria by recognizing the conserved moiety within the A1γ-type PG (Mikoulinskaia et al., 2009; Schleifer & Kandler, 1972). Two other *Bacillus*-targeting endolysins, LysB4 and LysPBC2, also showed the similar broad range including both Gram-positive and Gram-negative bacteria, although their CBDs (i.e., SH3_5 in LysB4 and two SH3_3 in LysPBC2) were different from that of LysBCC348, which is the SPOR domain (Kong et al., 2019; Son et al., 2012). Since the EAD of LysBCC348 showed a lower but significant lytic activity, it remains to be investigated whether the LysBCC348EAD is involved in the recognition of the A1γ-type PG.

Based on our results, phage BCC348 and endolysin LysBCC348 can be applied in various food processing environments to address issues of *B. cereus* contamination. Our findings suggest that they can be used as food additives during the production and storage of *B. cereus*-susceptible starchy foods, including *Garaetteok*, cooked rice, pasta, etc. Not only the direct treatment of food with the phage and endolysin, but also food packaging that may come into contact with the food, such as food absorbent pads, packaging films, and food containers, would be other attractive options where these two alternative antimicrobials could be incorporated (Gouvêa et al., 2015; Lee et al., 2024; Solanki et al., 2013). Development of hand sanitizers for food service employees, detergents for food processing equipment/facilities, and therapeutics for *B. cereus* infections is also feasible.

However, since we only demonstrated the activity of BCC348 and LysBCC348 *in vitro* and in artificially contaminated models, their practical utility in real-world applications needs to be further investigated in detail. The surrounding natural microbial members and complex noise substances on the control targets, which are difficult to mimic in artificial model experiments, may impact the efficacy and efficiency of BCC348 and LysBCC348's anti-*B. cereus* activity. Therefore, their appropriate optimal titer and concentration for each specific application should be determined in advance to maximize control efficiency. Additionally, the economic feasibility of such applications is another factor that should be carefully considered. Since the preparation of endolysins as enzybiotics via protein expression systems is relatively expensive, cost-effective production methods need to be developed to make them more accessible for the food industry. Human health concerns also represent a challenge, even though phages and endolysins are biological agents that specifically target bacteria. As shown in a recent first-in-human phase 1 clinical trial demonstrating the absence of serious adverse events after oral phage administration (Federici et al., 2022), further rigorous validation of phage safety could support their broader use in practical food environments.

Taken together, the present study suggests that the novel *Becedseptimavirus* genus phage BCC348 with superior host lysis activity and its partial SPOR domain-containing endolysin LysBCC348 could be promising candidates as alternative anti-*B. cereus* agents in the food industry. To enhance their effectiveness, consumer-friendliness, and safety for widespread use, further studies should focus on their practical applications and potential human health impact. In addition, further comprehensive analysis and engineering of the endolysin structure could improve its lytic activity and/or expand its target range for more efficient use under diverse food processing conditions.

CRediT authorship contribution statement

Hanbin Seol: Writing – original draft, Validation, Methodology, Investigation, Data curation. **Byoung Sik Kim:** Writing – review & editing, Visualization, Formal analysis. **Minsik Kim:** Writing – review & editing, Writing – original draft, Visualization, Supervision, Funding acquisition, Formal analysis, Conceptualization.

Funding

This work was supported by the "Cooperative Research Program for Agriculture Science and Technology Development [Project No. PJ01574702]," Rural Development Administration, South Korea; the Basic Science Research Programs [RS-2024-00348309] through the National Research Foundation of Korea (NRF), South Korea; the Korea Basic Science Institute (National research Facilities and Equipment Center) grant [RS-2024-00403831] funded by the Korea government (MSIT), South Korea.

Declaration of competing interest

The authors declare that they have no known competing financial interests or personal relationships that could have appeared to influence the work reported in this paper.

Acknowledgements

We would like to thank Prof. Sangryeol Ryu and Dr. Jinshil Kim of Seoul National University, South Korea, for their technical assistance with the TEM observations.

Appendix A. Supplementary data

Supplementary data to this article can be found online at https://doi.org/10.1016/j.lwt.2024.117034.

Data availability

Data will be made available on request.

References

Bottone, E. J. (2010). *Bacillus cereus*, a volatile human pathogen. *Clinical Microbiology Reviews, 23*(2), 382–398. https://doi.org/10.1128/CMR.00073-09

Chen, X. M., Gao, T. T., Peng, Q., Zhang, J., Chai, Y. R., & Song, F. P. (2018). Novel cell wall hydrolase CwlC from *Bacillus thuringiensis* is essential for mother cell lysis. *Applied and Environmental Microbiology, 84*(7), Article e02640. https://doi.org/10.1128/AEM.02640-17

Choi, H. J., & Kim, M. (2021). Improved bactericidal efficacy and thermostability of *Staphylococcus aureus*-specific bacteriophage SA3821 by repeated sodium pyrophosphate challenges. *Scientific Reports, 11*(1), Article 22951. https://doi.org/10.1038/s41598-021-02446-1

Criel, B., Taelman, S., Van Criekinge, W., Stock, M., & Briers, Y. (2021). PhaLP: A database for the study of phage lytic proteins and their evolution. *Viruses-Basel, 13*(7). https://doi.org/10.3390/v13071240

Dunne, M., Prokhorov, N. S., Loessner, M. J., & Leiman, P. G. (2021). Reprogramming bacteriophage host range: Design principles and strategies for engineering receptor binding proteins. *Current Opinion in Biotechnology, 68*, 272–281. https://doi.org/10.1016/j.copbio.2021.02.006

Endersen, L., & Coffey, A. (2020). The use of bacteriophages for food safety. *Current Opinion in Food Science, 36*, 1–8. https://doi.org/10.1016/j.cofs.2020.10.006

Federici, S., Kredo-Russo, S., Valdes-Mas, R., Kviatcovsky, D., Weinstock, E., Matiuhin, Y., Silberberg, Y., Atarashi, K., Furuichi, M., Oka, A., Liu, B., Fibelman, M., Weiner, I. N., Khabra, E., Cullin, N., Ben-Yishai, N., Inbar, D., Ben-David, H., Nicenboim, J., & Elinav, E. (2022). Targeted suppression of human IBD-associated gut microbiota commensals by phage consortia for treatment of intestinal inflammation. *Cell, 185*(16), 2879–2898. https://doi.org/10.1016/j.cell.2022.07.003. e2824.

Gibson, D. G., Young, L., Chuang, R. Y., Venter, J. C., Hutchison, C. A., & Smith, H. O. (2009). Enzymatic assembly of DNA molecules up to several hundred kilobases. *Nature Methods, 6*(5), 343. https://doi.org/10.1038/Nmeth.1318. U341.

Gouvêa, D. M., Mendonça, R. C. S., Soto, M. L., & Cruz, R. S. (2015). Acetate cellulose film with bacteriophages for potential antimicrobial use in food packaging. *LWT–Food Science and Technology, 63*(1), 85–91. https://doi.org/10.1016/j.lwt.2015.03.014

Grutsch, A. A., Nimmer, P. S., Pittsley, R. H., Kornilow, K. G., & McKillip, J. L. (2018). Molecular pathogenesis of *Bacillus* spp., with emphasis on the dairy industry. *Fine Focus, 4*(2), 203–222. https://doi.org/10.33043/FF.4.2.203-222

Huang, Y., Flint, S. H., & Palmer, J. S. (2020). *Bacillus cereus* spores and toxins - the potential role of biofilms. *Food Microbiology, 90*, Article 103493. https://doi.org/10.1016/j.fm.2020.103493

Huang, Z., Yuan, X., Zhu, Z., Feng, Y., Li, N., Yu, S., Li, C., Chen, B., Wu, S., Gu, Q., Zhang, J., Wang, J., Wu, Q., & Ding, Y. (2024). Isolation and characterization of *Bacillus cereus* bacteriophage DZ1 and its application in foods. *Food Chemistry, 431*, Article 137128. https://doi.org/10.1016/j.foodchem.2023.137128

Hutinet, G., Kot, W., Cui, L., Hillebrand, R., Balamkundu, S., Gnanakalai, S., Neelakandan, R., Carstens, A. B., Fa Lui, C., Tremblay, D., Jacobs-Sera, D., Sassanfar, M., Lee, Y. J., Weigele, P., Moineau, S., Hatfull, G. F., Dedon, P. C., Hansen, L. H., & de Crecy-Lagard, V. (2019). 7-Deazaguanine modifications protect phage DNA from host restriction systems. *Nature Communications, 10*(1), 5442. https://doi.org/10.1038/s41467-019-13384-y

Kim, G., Kim, J. H., & Kim, M. (2023). Potential of bacteriophage PCT27 to reduce the use of agrochemicals to control *Pectobacterium carotovorum* subsp. *carotovorum* in Chinese cabbage (*Brassica pekinensis*). *Food Control, 154*, Article 109985. https://doi.org/10.1016/j.foodcont.2023.109985

Kim, D., Kim, J., & Kim, M. (2024). Potential of antimicrobial peptide-fused endolysin LysC02 as therapeutics for infections and disinfectants for food contact surfaces to control *Cronobacter sakazakii*. *Food Control, 157*, Article 110190. https://doi.org/10.1016/j.foodcont.2023.110190

Kim, H., Moon, M. J., Kim, C. Y., & Ryu, K. (2019). Efficacy of chemical sanitizers against *Bacillus cereus* on food contact surfaces with scratch and biofilm. *Food Science and Biotechnology, 28*(2), 581–590. https://doi.org/10.1007/s10068-018-0482-2

Kim, M., & Ryu, S. (2011). Characterization of a T5-like coliphage, SPC35, and differential development of resistance to SPC35 in *Salmonella enterica* serovar Typhimurium and *Escherichia coli*. *Applied and Environmental Microbiology, 77*(6), 2042–2050. https://doi.org/10.1128/AEM.02504-10

Kong, M., Na, H., Ha, N. C., & Ryu, S. (2019). LysPBC2, a novel endolysin harboring a *Bacillus cereus* spore binding domain. *Applied and Environmental Microbiology, 85*(5), Article e02462. https://doi.org/10.1128/AEM.02462-18

Kong, M., Sim, J., Kang, T., Nguyen, H. H., Park, H. K., Chung, B. H., & Ryu, S. (2015). A novel and highly specific phage endolysin cell wall binding domain for detection of *Bacillus cereus*. *European Biophysics Journal, 44*(6), 437–446. https://doi.org/10.1007/s00249-015-1044-7

Ku, S. K., Hong, J. S., Choi, H. D., Park, J. D., Kim, Y. B., Choi, H. W., Kim, T. K., & Choi, Y. S. (2018). A study of the quality characteristics of frozen Korean rice cake by using different thawing methods. *Food Science and Biotechnology, 27*(5), 1343–1351. https://doi.org/10.1007/s10068-018-0376-3

Lee, W. J., Billington, C., Hudson, J. A., & Heinemann, J. A. (2011). Isolation and characterization of phages infecting *Bacillus cereus*. *Letters in Applied Microbiology, 52*(5), 456–464. https://doi.org/10.1111/j.1472-765X.2011.03023.x

Lee, J., Kim, D., & Kim, M. (2023). The application of adaptively evolved thermostable bacteriophage ΦYMFM0293 to control *Salmonella* spp. in poultry skin. *Food Research International, 167*, Article 112665. https://doi.org/10.1016/j.foodres.2023.112665

Lee, C., Kim, H., & Ryu, S. (2023). Bacteriophage and endolysin engineering for biocontrol of food pathogens/pathogens in the food: Recent advances and future trends. *Critical Reviews in Food Science and Nutrition, 63*(27), 8919–8938. https://doi.org/10.1080/10408398.2022.2059442

Lee, I., Lee, J., & Kim, M. (2024). Inhibition of *Salmonella* growth in exudates drained from poultry meat by bacteriophage cocktail-containing absorbent food pad. *LWT–Food Science and Technology, 197*, Article 115908. https://doi.org/10.1016/j.lwt.2024.115908

Lee, J. H., Shin, H., & Ryu, S. (2014). Characterization and comparative genomic analysis of bacteriophages infecting members of the *Bacillus cereus* group. *Archives of Virology, 159*(5), 871–884. https://doi.org/10.1007/s00705-013-1920-3

Li, N., Yuan, X. M., Li, C., Chen, N., Wang, J., Chen, B., Yu, S. B., Yu, P. F., Zhang, J. H., Zeng, H. Y., Wu, S., Yang, X. J., Yang, M. Y., Zhang, J. M., Wu, Q. P., & Ding, Y. (2022). A novel bacteriophage DLn1 and its endolysin as biocontrol agents against in milk. *International Journal of Food Microbiology, 369*, Article 109615. https://doi.org/10.1016/j.ijfoodmicro.2022.109615

Liu, H., Hu, Z., Li, M. Y., Yang, Y., Lu, S. G., & Rao, X. C. (2023). Therapeutic potential of bacteriophage endolysins for infections caused by Gram-positive bacteria. *Journal of Biomedical Science, 30*(1), Article 29. https://doi.org/10.1186/s12929-023-00919-1

Liu, X., Zhang, R., Hou, S., Liu, H., Wang, J., Yu, Q., Peng, Q., & Song, F. (2021). Identification and functional characterization of two homologous SpoVS proteins involved in sporulation of *Bacillus thuringiensis*. *Microbiology Spectrum, 9*(2), Article e00881. https://doi.org/10.1128/Spectrum.00881-21

Loc-Carrillo, C., & Abedon, S. T. (2011). Pros and cons of phage therapy. *Bacteriophage, 1*(2), 111–114. https://doi.org/10.4161/bact.1.2.14590

Marongiu, L., Burkard, M., Lauer, U. M., Hoelzle, L. E., & Venturelli, S. (2022). Reassessment of historical clinical trials supports the effectiveness of phage therapy. *Clinical Microbiology Reviews, 35*(4). https://doi.org/10.1128/cmr.00062-22

Mikoulinskaia, G. V., Odinokova, I. V., Zimin, A. A., Lysanskaya, V. Y., Feofanov, S. A., & Stepnaya, O. A. (2009). Identification and characterization of the metal ion-dependent L-alanoyl-D-glutamate peptidase encoded by bacteriophage T5. *FEBS Journal, 276*(24), 7329–7342. https://doi.org/10.1111/j.1742-4658.2009.07443.x

Mishima, M., Shida, T., Yabuki, K., Kato, K., Sekiguchi, J., & Kojima, C. (2005). Solution structure of the peptidoglycan binding domain of *Bacillus subtilis* cell wall lytic enzyme CwlC: Characterization of the sporulation-related repeats by NMR. *Biochemistry, 44*(30), 10153–10163. https://doi.org/10.1021/bi050624n

Monk, A. B., Rees, C. D., Barrow, P., Hagens, S., & Harper, D. R. (2010). Bacteriophage applications: Where are we now? *Letters in Applied Microbiology, 51*(4), 363–369. https://doi.org/10.1111/j.1472-765X.2010.02916.x

Okshevsky, M., Louw, M. G., Lamela, E. O., Nilsson, M., Tolker-Nielsen, T., & Meyer, R. L. (2018). A transposon mutant library of *Bacillus cereus* ATCC 10987 reveals novel genes required for biofilm formation and implicates motility as an important factor for pellicle-biofilm formation. *Microbiologica, 7*(2), Article e552. https://doi.org/10.1002/mbo3.552

Oliveira, H., Melo, L. D., Santos, S. B., Nobrega, F. L., Ferreira, E. C., Cerca, N., Azeredo, J., & Kluskens, L. D. (2013). Molecular aspects and comparative genomics

of bacteriophage endolysins. *Journal of Virology, 87*(8), 4558–4570. https://doi.org/10.1128/JVI.03277-12

Ouyang, R., Ongenae, V., Muok, A., Claessen, D., & Briegel, A. (2024). Phage fibers and spikes: A nanoscale Swiss army knife for host infection. *Current Opinion in Microbiology, 77*, Article 102429. https://doi.org/10.1016/j.mib.2024.102429

Park, H. W., & Yoon, W. B. (2019). A quantitative microbiological exposure assessment model for *Bacillus cereus* in pasteurized rice cakes using computational fluid dynamics and Monte Carlo simulation. *Food Research International, 125*, Article 108562. https://doi.org/10.1016/j.foodres.2019.108562

Resnekov, O., Driks, A., & Losick, R. (1995). Identification and characterization of sporulation gene spoVS from *Bacillus subtilis*. *Journal of Bacteriology, 177*(19), 5628–5635. https://doi.org/10.1128/jb.177.19.5628-5635.1995

Schleifer, K. H., & Kandler, O. (1972). Peptidoglycan types of bacterial cell walls and their taxonomic implications. *Bacteriological Reviews, 36*(4), 407–477. https://doi.org/10.1128/br.36.4.407-477.1972

Schmelcher, M., & Loessner, M. J. (2016). Bacteriophage endolysins: Applications for food safety. *Current Opinion in Biotechnology, 37*, 76–87. https://doi.org/10.1016/j.copbio.2015.10.005

Solanki, K., Grover, N., Downs, P., Paskaleva, E. E., Mehta, K. K., Lee, L., Schadler, L. S., Kane, R. S., & Dordick, J. S. (2013). Enzyme-based listericidal nanocomposites. *Scientific Reports, 3*, Article 1584. https://doi.org/10.1038/srep01584

Son, B., Yun, J., Lim, J. A., Shin, H., Heu, S., & Ryu, S. (2012). Characterization of LysB4, an endolysin from the *Bacillus cereus*-infecting bacteriophage B4. *BMC Microbiology, 12*(33), Article 33. https://doi.org/10.1186/1471-2180-12-33

Song, X., Bredahl, L., Navarro, M. D., Pendenza, P., Stojacic, I., Mincione, S., Pellegrini, G., Schlüter, O. K., Torrieri, E., Di Monaco, R., & Giacalone, D. (2022). Factors affecting consumer choice of novel non-thermally processed fruit and vegetables products: Evidence from a 4-country study in Europe. *Food Research International, 153*, Article 110975. https://doi.org/10.1016/j.foodres.2022.110975

Stenfors Arnesen, L. P., Fagerlund, A., & Granum, P. E. (2008). From soil to gut: *Bacillus cereus* and its food poisoning toxins. *FEMS Microbiology Reviews, 32*(4), 579–606. https://doi.org/10.1111/j.1574-6976.2008.00112.x

Strathdee, S. A., Hatfull, G. F., Mutalik, V. K., & Schooley, R. T. (2023). Phage therapy: From biological mechanisms to future directions. *Cell, 186*(1), 17–31. https://doi.org/10.1016/j.cell.2022.11.017

Tan, S., Chen, H., Huang, S., Zhu, B., Wu, J., Chen, M., Zhang, J., Wang, J., Ding, Y., Wu, Q., & Yang, M. (2024). Characterization of the novel phage vB_BceP_LY3 and its potential role in controlling *Bacillus cereus* in milk and rice. *International Journal of Food Microbiology, 421*, Article 110778. https://doi.org/10.1016/j.ijfoodmicro.2024.110778

Thiaville, J. J., Kellner, S. M., Yuan, Y. F., Hutinet, G., Thiaville, P. C., Jumpathong, W., Mohapatra, S., Brochier-Armanet, C., Letarov, A. V., Hillebrand, R., Malik, C. K., Rizzo, C. J., Dedon, P. C., & de Crécy-Lagard, V. (2016). Novel genomic island modifies DNA with 7-deazaguanine derivatives. *Proceedings of the National Academy of Sciences of the United States of America, 113*(11), E1452–E1459. https://doi.org/10.1073/pnas.1518570113

Wan, X., Geng, P., Sun, J., Yuan, Z., & Hu, X. (2021). Characterization of two newly isolated bacteriophages PW2 and PW4 and derived endolysins with lysis activity against *Bacillus cereus* group strains. *Virus Research, 302*, Article 198489. https://doi.org/10.1016/j.virusres.2021.198489

Weigele, P., & Raleigh, E. A. (2016). Biosynthesis and function of modified bases in bacteria and their viruses. *Chemical Reviews, 116*(20), 12655–12687. https://doi.org/10.1021/acs.chemrev.6b00114

Wilcox, S. A., Toder, R., & Foster, J. W. (1996). Rapid isolation of recombinant lambda phage DNA for use in fluorescence in situ hybridization. *Chromosome Research, 4*(5), 397–398. https://doi.org/10.1007/BF02257276

Williams, K. B., Yahashiri, A., Arends, S. J. R., Popham, D. L., Fowler, C. A., & Weiss, D. S. (2013). Nuclear magnetic resonance solution structure of the peptidoglycan-binding SPOR domain from *Escherichia coli* DamX: Insights into septal localization. *Biochemistry, 52*(4), 627–639. https://doi.org/10.1021/bi301609e

Yahashiri, A., Jorgenson, M. A., & Weiss, D. S. (2015). Bacterial SPOR domains are recruited to septal peptidoglycan by binding to glycan strands that lack stem peptides. *Proceedings of the National Academy of Sciences of the United States of America, 112*(36), 11347–11352. https://doi.org/10.1073/pnas.1508536112

Yahashiri, A., Jorgenson, M. A., & Weiss, D. S. (2017). The SPOR domain, a widely conserved peptidoglycan binding domain that targets proteins to the site of cell division. *Journal of Bacteriology, 199*(14), Article e00118. https://doi.org/10.1128/JB.00118-17

Zhang, Y. F., Huber, N., Moeller, R., Stülke, J., Dubovcova, B., Akepsimaidis, G., Meneses, N., Drissner, D., & Mathys, A. (2020). Role of DNA repair in spore resistance to high energy and low energy electron beam treatments. *Food Microbiology, 87*, Article 103353. https://doi.org/10.1016/j.fm.2019.103353

Zhao, L., Duan, F., Gong, M., Tian, X., Guo, Y., Jia, L., & Deng, S. (2021). (+)-Terpinen-4-ol inhibits *Bacillus cereus* biofilm formation by upregulating the interspecies quorum sensing signals diketopiperazines and diffusing signaling factors. *Journal of Agricultural and Food Chemistry, 69*(11), 3496–3510. https://doi.org/10.1021/acs.jafc.0c07826